

Multifunctional Hemostatic PVA/Chitosan Sponges Loaded with Hydroxyapatite and Ciprofloxacin

Saif El-Din Al-Mofty, Ali H. Karaly, Wessam Awad Sarhan,* and Hassan M. E. Azzazy*

Cite This: *ACS Omega* 2022, 7, 13210–13220

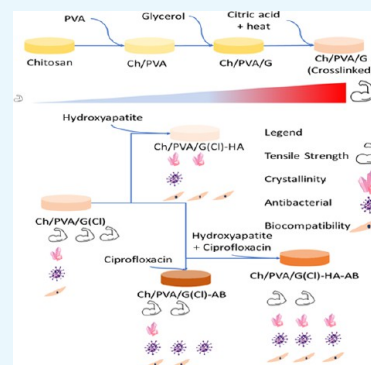
Read Online

ACCESS |

Metrics & More

Article Recommendations

ABSTRACT: The present study describes the development of multifunctional hemostatic sponges to control bleeding. Chitosan (Ch) and poly(vinyl alcohol) (PVA) were selected as the basic polymeric matrix [Ch/PVA] for sponges. Glycerol and citric acid were used as crosslinkers [Ch/PVA/G(CI)] to enhance the mechanical properties of the developed sponges. Ciprofloxacin (AB) was added to the developed sponge to impart antibacterial activity. Hydroxyapatite (HA) was also added, which would make the sponge suitable for bone surgery. Among the developed sponges, the Ch/PVA/G(CI)-HA-AB sponge demonstrated enhanced cell viability, mechanical properties, and strong antimicrobial effect against *Escherichia coli*, *Pseudomonas aeruginosa*, and *Staphylococcus aureus*, in addition to platelet aggregation activity. The addition of ciprofloxacin and hydroxyapatite promotes a unique synergistic effect of antimicrobial activity and hemostasis. Thus, the present study introduces Ch/PVA/G(CI)-HA-AB, a multifunctional hemostatic sponge that would be suitable for bone surgical applications.



INTRODUCTION

Hemorrhage may cause hypoperfusion, acute ischemia, and disseminated intravascular coagulation, and in severe cases, it may cause hypovolemic shock, organ failure, and death. Prehospital mortality rates due to hemorrhage account for 35%.¹ Such high rates can be avoided if hemostasis is achieved with a minimal loss of blood and perfusion to the tissue that is affected. In this regard, hemostatic sponges and dressings are the most important and effective tools in managing hemostasis.

It is important to tailor hemostatic materials to suit certain needs at the hemorrhagic site in different cases such as bone surgery and dentistry.² Additionally, it is recommended that the hemostatic material should be nonimmunogenic and have antibacterial effects to avoid sepsis.^{2–5}

Many sponges were developed to achieve hemostasis and wound healing.^{5,6} Chitosan is an important polymer in hemostatic applications due to its anti-inflammatory properties, biocompatibility, and in vivo degradation.^{2,7} Chitosan exhibits excellent wettability and high absorption ability, in addition to its ability to promote the aggregation of the negatively charged red blood cells due to its protonated structure. However, chitosan exhibits poor mechanical properties^{7–9} and thus needs to be combined with other biocompatible synthetic polymers, such as poly(vinyl alcohol) (PVA), to improve the mechanical properties and functionality of the hemostatic sponge.^{10,11} In this study, we mixed chitosan, PVA, and glycerol. PVA exhibits several properties such as biodegradability, low toxicity, good mechanical properties, and high water absorption ability. Glycerol, on the other hand, improves the flexibility of the sponge, as well as its wettability.^{12–14} To

optimize the mechanical integrity, crosslinking of the sponges was performed using citric acid as a crosslinker via the esterification reaction that occurs between the carboxyl groups on citric acid and the hydroxyl groups on PVA and glycerol.¹⁵

To develop a multifunctional hemostatic sponge for bone surgery applications, the PVA/chitosan sponge was further loaded with hydroxyapatite (HA) and ciprofloxacin. Hydroxyapatite is widely utilized for its bone regenerative capabilities. It is a naturally existing mineral that exists as a hexagonal crystal of calcium, oxygen, and phosphorus. It was demonstrated that when the hydroxyapatite is incorporated into hemostatic agents, it promotes osteogenic differentiation.^{16–18} HA was also reported to have antimicrobial activity due to its high concentration of calcium ions, which increases the probability of its uptake by the bacteria and thus induces calcium stress that initiates signaling for bacterial death. However, a few bacteria exhibit a defense mechanism that can efflux the Ca^{2+} ions through calcium-binding proteins or stored in vesicles at the outer-surface membrane of the bacteria.¹⁹

Ciprofloxacin is a broad-spectrum antibiotic from the tetracycline family of antibiotics that have been used for endodontic infections.²⁰ For dental surgeries, ciprofloxacin is

Received: February 1, 2022

Accepted: March 23, 2022

Published: April 11, 2022



the first line of defense against microbial infections.^{21,22} However, due to antibiotic abuse, several bacterial strains have developed resistance to ciprofloxacin due to mutations in the GyrA gene, the gene responsible for topoisomerase II in several bacterial strains, in addition to the ability of these bacterial strains to efflux the antibiotic from the cell membrane.^{21,22} Thus, within the current work, HA was combined with ciprofloxacin and tested for their synergetic antibacterial activity within the developed chitosan/PVA sponges, which were optimized to serve as a multifunctional hemostatic sponge for bone surgery applications.

MATERIALS AND METHODS

Chitosan with a molecular weight of 240,000 and a degree of deacetylation of 84% was obtained from Primex, Iceland. Glacial acetic acid and poly(vinyl alcohol) (M_w 85,000) were obtained from Oxford, U.K. Anhydrous citric acid, glycerol, calcium chloride, sodium dibasic phosphate, ammonium oxalate, Leishman stain, ciprofloxacin, and glass petri dish were obtained from a local vendor. Tryptic soy broth was obtained from NEOGEN, U.K. Agar-agar was obtained from B&V, Italy. Phosphate buffer saline, Dulbecco's minimal Eagle medium (DMEM), L-glutamine, penicillin–streptomycin 100×, trypsin-EDTA, and fetal bovine serum (FBS) were obtained from Lonza, Switzerland. 3-(4,5-Dimethylthiazol-2-yl)-2,5-diphenyltetrazolium (MTT) was obtained from SERVA, Germany. Sodium hydroxide was obtained from Sigma, Germany. Dimethyl sulfoxide (DMSO) and glycerol (Gly) were obtained from Fisher U.K., and 96-well F-bottom plates were obtained from Greiner, Austria. T75 flasks were obtained from Corning, USA. Thermogravimetric analyzer (TA Instruments, New Castle, Delaware), Fourier transform infrared spectrometer (FTIR; Thermo Fisher, Waltham, Massachusetts), shaking incubator (JSR JSSI-100T, Korea), biosafety cabinet (JSR, Korea), CO₂ incubator (NuAire, Plymouth, Minnesota), incubator (BTC, local vendor), Instron 3342, inverted phase-contrast microscope (Olympus, Tokyo, Japan), and Omega FLOUstar (BMG LABTECH, Germany) were purchased.

Hydroxyapatite Synthesis. Hydroxyapatite was prepared according to the literature with slight modifications.²³ Briefly, 9 g of CaCl₂ and 8 g of Na₂HPO₄ were mixed slowly in 400 mL of distilled water, and then 2 mL of 2 M NaOH was added dropwise. The hydroxyapatite (HA) is formed from the clear mixture as a white precipitate, and then HA was washed twice with distilled water by decantation. The samples were then filtered and left to dry under ambient temperature.

Preparation of the Chitosan/PVA Sponges Loaded with Hydroxyapatite and Ciprofloxacin. Chitosan (Ch; 1% (w/v)) was dissolved in 0.5% acetic acid, and then 1% (w/v) PVA and 15% (w/w of PVA) of anhydrous citric acid were added to the solution. Lastly, Gly was added to the final weight ratio of Cs/PVA/Gly of 1:1:2. To enhance the antibacterial property of the sponge, 10% of the total polymer of ciprofloxacin was added to the final solution. Moreover, 10% of the total polymer of HA was added to the final solution and stirred well until homogeneity was achieved and placed in the bath sonicator for degassing for 5 min. The solutions were freeze-dried and then thermally crosslinked (Cl) at 110 °C for 10 min and then packed in sealed plastic bags.

Tensile Strength (TS) of Ch/PVA/G(Cl) Sponges and their Derivatives. The mechanical properties of sponges were tested using the Universal Testing Machine (UTM) with

100 newton (N) load cells. Sponges were cut into rectangular-shaped (10 cm × 0.5 cm) strips, and their ends were clamped with the steel grip jaws of a UTM instrument for the measurement. The percentage of elongation is derived from eq 1

$$\% \delta = (\text{length final} - \text{length initial}) / \text{length initial} \quad (1)$$

Characterization of the Ch/PVA/G(Cl) Sponges and their Derivatives. The sponges were cut into squares, and the squares were further cut into traverse sections and placed on carbon tapes on the side of the sponge showing the porosity of the sponges; the images were taken without sputtering. Scanning electron microscopy (SEM) was performed under high vacuum, and the electron beam was set at 5 kV.

The images were further analyzed using Image J using a simple threshold in an 8-bit jpg format. The results of the area of porosity were further analyzed in R studio (version 4.0.1). The area of the porous structure is assumed to be circular, and hence the diameter is calculated as follows

$$\text{diameter} = \text{square root} (\pi \times \text{area} / 4) \quad (2)$$

24

The sponges were cut into disks of 3.5 cm in diameter and placed on the sample holder of the X-ray diffraction (XRD) instrument and 2θ values ranging from 5 to 60° were measured. The graph was plotted using Origin version 8.0.

The functional groups of the sponges were scanned (400–4500 cm⁻¹) using an FTIR with an attenuated total reflection (ATR) accessory with a resolution of 2 cm⁻¹. The graph data points were computed in the Origin program.

Thermal degradation of the sponges was obtained via thermogravimetric analysis by adding 10–15 mg of each sponge type on a platinum pan and calculating the retained mass after heating from ambient temperature to 210 °C under nitrogen gas. The data points were smoothed using LOESS.^{25–27}

Evaluation of Swelling and Degradation. The sponges were cut into small masses (10–20 mg) and placed in each well of a 24-well plate containing 1 mL of phosphate-buffered saline (PBS) pH 7.4 w/o Ca⁺²/Mg⁺². Sponge mass was measured after lightly blotting with filter paper to remove damped water. Degradation was performed with the same apparatus, but the sponges were dried completely and then weighed after 1, 3, 5, and 10 days.

Antimicrobial Evaluation of the Ch/PVA/G(Cl) Sponges and their Derivatives. The antibacterial activity of the chitosan sponges was tested against *Escherichia coli*, *Staphylococcus aureus*, and *Pseudomonas aeruginosa*, using the disk diffusion method according to ISO 20645:2004 for antibacterial efficiency with the disk diffusion method. Briefly, using an overnight culture of each bacterial strain, the bacterial strains were diluted using the 0.5 McFarland standard in 10 mL of broth. The bacterial cells were spread on agar plates (9 cm), and the disks were placed either as a whole disk or cut in halves or in quarters. The plates were placed inverted in the incubator and left overnight, and then inhibition zones were assessed. The area of the inhibition zone was calculated using Image J. The diameter was then calculated according to eq 2.²⁴

Evaluation of the Hemostatic Ability of the Ch/PVA/G(Cl) Sponges and Their Derivatives. The chitosan sponges Ch/PVA, Ch/PVA/AB, Ch/PVA/HA, and Ch/PVA/HA/AB were evaluated for their hemostatic ability

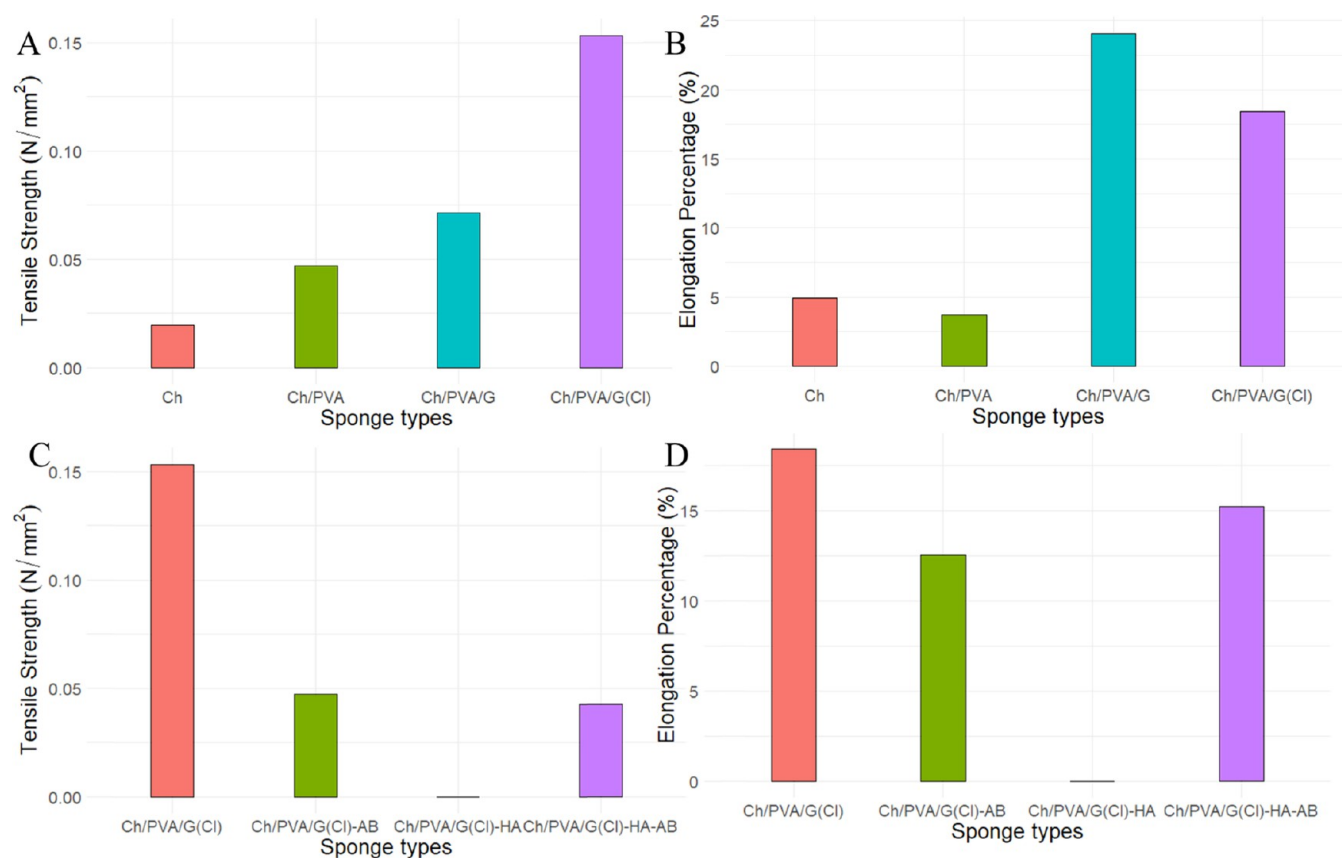


Figure 1. (A) Tensile strength of Ch, Ch/PVA, Ch/PVA/G, and Ch/PVA/G(Cl) and (B) their respective percentage elongations. (C and D) Percentage of elongation of chitosan sponges.

utilizing a qualitative method using blood smear aggregation and a quantitative method of platelet count aggregation.

One hundred microliters of whole blood from a blood bank was placed on a glass slide. The chitosan/PVA sponges were placed on top of the blood and left for 3 min. The slide was then smeared and left to dry. Absolute ethanol was utilized as a fixing media for 5 min. Leishman stain was used to cover the whole slide for 15 min and then washed with tap water and left to dry. The micrograph images were taken with an Olympus microscope at 10 \times magnification.

For quantification of platelet aggregation, 100 μ L of serum was added to each well. The chitosan/PVA sponges were cut into 0.5 \times 0.5 cm² pieces, sterilized, and placed in each well for 3 min, and platelet count at 0, 1, and 3 min was obtained. Ten microliters of the sample was aspirated at each time point and placed in 1% ammonium oxalate (1:19) and left for 5 min. Then, 10 μ L was loaded into hemocytometer chambers and left for 15 min in a humidified chamber. Platelets were counted in both chambers at each time point. The platelets were counted and calculated as follows

$$\text{platelet per mL} = \text{platelet count} / 5 \times 1/0.2 \times 2000 \quad (3)$$

Cytotoxicity Study. Sponge disks were cut into 1–2 mm in thickness and 5.5 mm in diameter. The disks were sterilized on each side by exposure to UV for 20 min. The disks were soaked in warm maintenance media for 24 h (DMEM high glucose, 2% FBS, 100 U/mL of penicillin–streptomycin, and 1 \times of L-glutamine). L929 cells were seeded at a cell density of 10,000 cells/well and incubated for 24 h in a 96-well plate with a complete medium (DMEM high glucose, 10% FBS, 100 U/

mL of penicillin–streptomycin, and 1 \times of L-glutamine). The media was replaced with the preconditioned media and incubated for 24 h. An MTT solution (10 mg/mL) was added to 10% of the volume of the well plate incubated for 3 h, and then the solution was discarded, leaving the insoluble formazan to be dissolved in 100 μ L of DMSO. The plate was incubated for 15 min with gentle rocking and read using a plate reader at 570 nm.

Statistical Analysis. All statistical analyses were performed using the R program (R studio). For multiple mean comparisons, the Kruskal–Wallis test was used, followed by the Dunn test.

RESULTS AND DISCUSSION

Mechanical Properties of Ch/PVA/G(Cl) Sponges. The tensile strength and percent elongation values of the fabricated sponges with different compositions are shown in Figure 1. The plain chitosan sponge exhibited the least tensile strength value and the lowest percent of elongation due to its inherent mechanical properties. Upon addition of the PVA to Ch, the tensile strength was improved due to hydrogen bond formation between the positive charges of the amine groups in chitosan and the hydroxyl groups of PVA,²⁸ however, the percent of elongation was not improved. Thus, glycerol was added as a plasticizer within the Ch/PVA/G to increase the elongation percentage. As shown in Figure 1B, the addition of glycerol resulted in a dramatic increase in the elongation percentage from 5% of the Ch/PVA to 25% of the Ch/PVA/G. Additionally, glycerol is a small molecule that can diffuse between the larger polymer and hence increase hydrogen

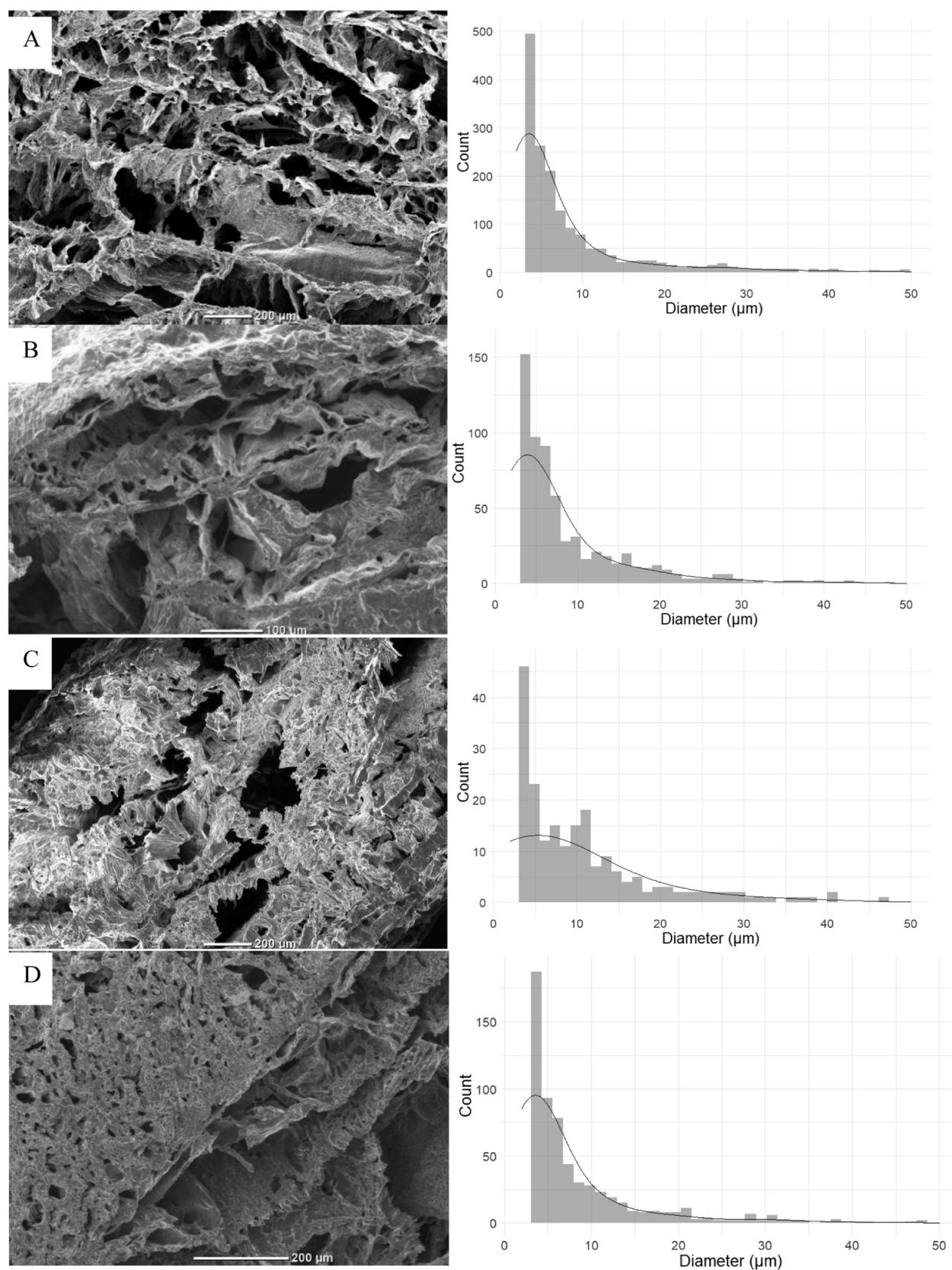


Figure 2. SEM images showing the microscopic structure with their histogram plot showing the pore diameter captured with Image J analysis: (A) Ch/PVA/G(Cl), (B) Ch/PVA/G(Cl)-AB, (C) Ch/PVA/G(Cl)-HA, and (D) Ch/PVA/G(Cl)-HA-AB.

bonding with chitosan; thus, it results in an increase in the tensile strength of the sponge.^{29,30} Lastly, the thermal crosslinking of PVA with citric acid in Ch/PVA/G(Cl) has

allowed the maximum increase in the tensile strength within Ch, Ch/PVA, and Ch/PVA/G sponges. However, the elongation percentage decreased to 18% due to the cross-

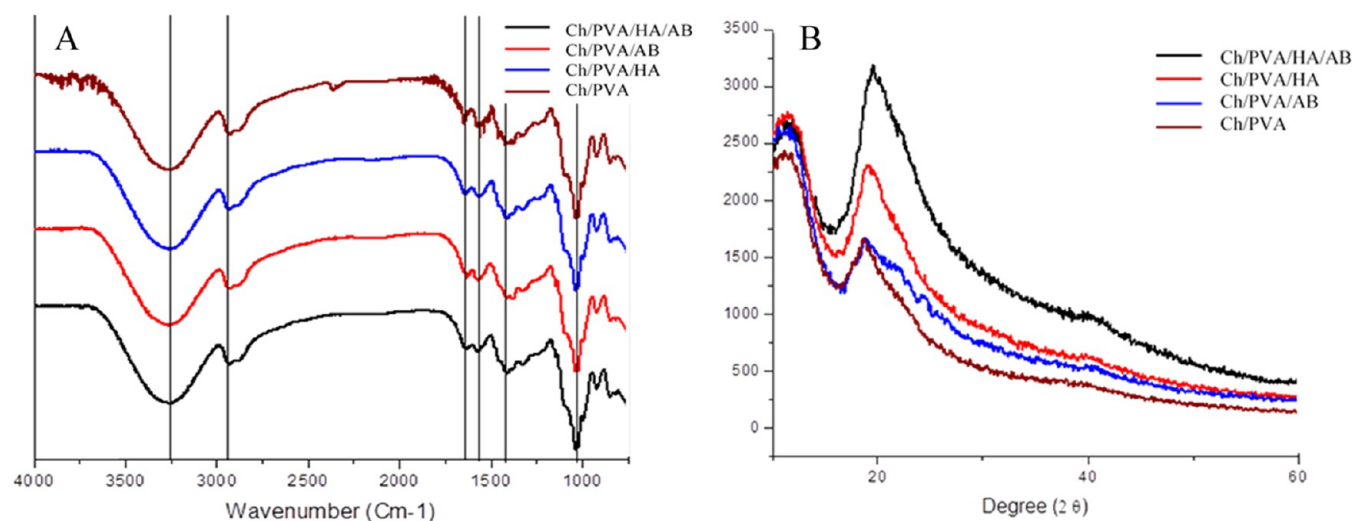


Figure 3. (A) FTIR spectrum of Ch/PVA/G(Cl), Ch/PVA/G(Cl)-AB, Ch/PVA/G(Cl)-HA, and Ch/PVA/G(Cl)-HA-AB. (B) X-ray diffraction patterns for chitosan/PVA, Ch/PVA/HA, Ch/PVA/AB, and Ch/PVA/HA/AB sponges.

linking of the lattice structure of the polymeric network and thus restricted the movement of the polymers.³¹ Consequently, Ch/PVA/G(Cl) was selected to be utilized in the rest of the study as the basic multifunctional hemostatic sponge due to its maximum tensile strength and a comparable percentage of elongation.

The Ch/PVA/G(Cl) sponges were loaded with ciprofloxacin (AB) and/or hydroxyapatite (HA). It was observed that the addition of ciprofloxacin (AB) within the Ch/PVA/G(Cl)-AB reduced the tensile strength by 3-fold in comparison to Ch/PVA/G(Cl) and reduced the percentage of elongation by almost half. This decrease in mechanical properties is due to the disturbance of homogeneity of the lattice structure by the antibiotic molecules. This is also clear in Ch/PVA/G(Cl)-HA, where the mechanical properties were reduced to zero for both elasticity and tensile strength due to the presence of Ca^{2+} ions in the matrix, which disrupted the lattice structure of the polymers.³²

However, the combination of HA and AB in Ch/PVA/G(Cl)-HA-AB resulted in tensile strength and elasticity similar to those in Ch/PVA/G(Cl)-AB. This is due to ciprofloxacin's ability to chelate Ca^{2+} ions, thus canceling its negative impact on the mechanical properties (Figure 2).^{33–35}

Characterization of the Developed Sponges. The sponges were analyzed for their morphological structure using a benchtop scanning electron microscope. The pore number in the descending order of the sponges is as follows: Ch/PVA/G(Cl) > Ch/PVA/G(Cl)-HA-AB > Ch/PVA/G(Cl)-AB > Ch/PVA/G(Cl)-HA. The pore size/diameter in all sponges ranged between 2.3 and 60 μm . The Ch/PVA/G(Cl)-HA exhibited the least number of pores.

The developed sponges were tested for their crystallinity via XRD. As shown in Figure 3, all of the tested samples had an amorphous pattern with observed peaks at 2θ values of 11 and 20°, which are characteristic of chitosan.²³ It can be observed that the Ch/PVA/G(Cl)-HA-AB sample had relatively higher crystallinity. This could be attributed to the ability of ciprofloxacin to chelate calcium ions from the hydroxyapatite, which upon freeze-drying may make a sort of a crystalline pattern.³⁶

The FTIR graph shows that the representative peaks of the hydroxyl group overlapped with amine group stretching

vibrations around $\nu 3255\text{ cm}^{-1}$, followed by CH_2 stretching at $\nu 2930\text{ cm}^{-1}$, which are present in the main scaffold. The primary amine peak as well as C=O and C–O stretching vibrations were observed at 1580, 1640, and 1400 respectively. In addition, the peak at 1030 cm^{-1} is characteristic of the C–N stretching vibration.^{33,37}

The developed sponges were tested for their thermal stability. As shown in Figure 4, the Ch/PVA/G(Cl) sponges

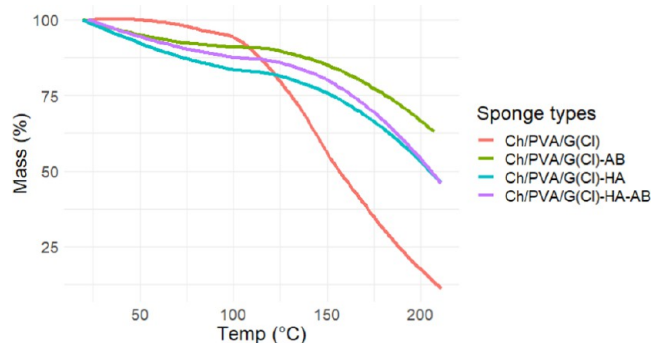


Figure 4. TGA graphs of the four sponges show that sponges containing ciprofloxacin had the highest thermal stability, while those of the blank showed the lowest thermal stability. The graph was smoothed through LOESS.

had the least thermal stability, retaining only 25% at 174 °C. Ch/PVA/G(Cl)-AB demonstrated greater thermal stability, retaining 65% of its mass at 210 °C, while Ch/PVA/G(Cl)-HA and Ch/PVA/G(Cl)-HA-AB retained 50% of their mass at 202 °C. This greater thermal stability in Ch/PVA/G(Cl)-AB could be attributed to the high melting point of ciprofloxacin, which increased the thermal stability of the Ch/PVA/G(Cl)-AB sponge; such a pattern has been detailed by Turel and Bukovec.³⁸ Such an effect was also observed in the Ch/PVA/G(Cl)-HA-AB; however, due to the presence of HA at 200 °C, the thermal stability decreased compared to that of Ch/PVA/G(Cl)-HA. The data obtained were smoothed using locally estimated scatterplot smoothing (LOESS) as the data points represented ~ 1000 observations.²⁵

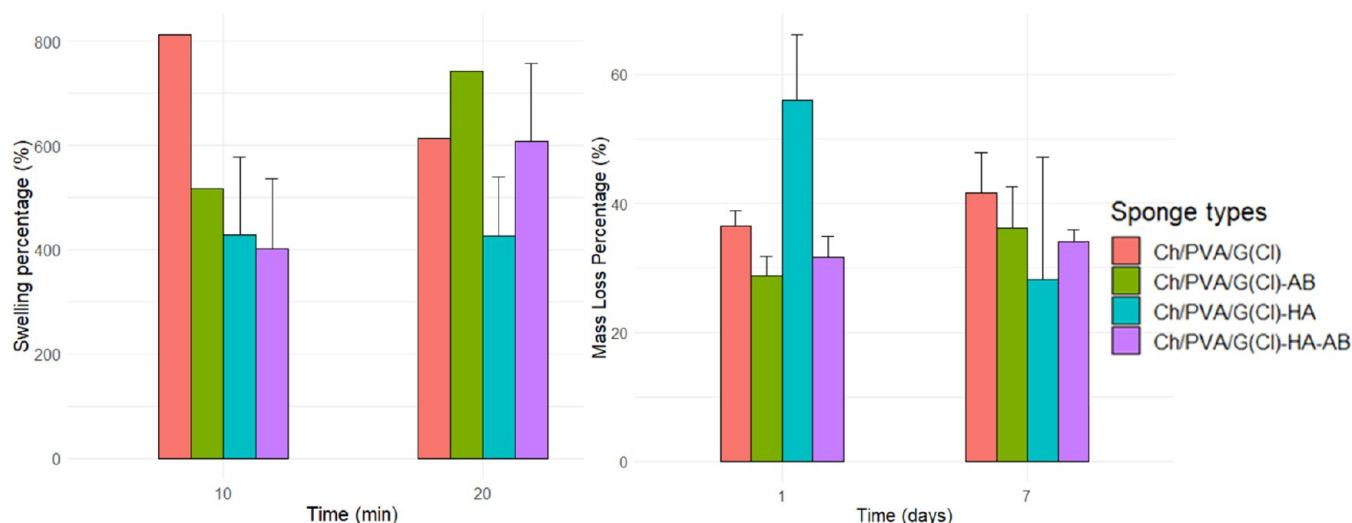


Figure 5. Swelling of chitosan sponges within 20 min and degradation for 7 days. The sponges were kept in PBS pH 7.4, incubated at 37 °C, and then weighed after the removal of water from the surface of the sponge disks. The error bars represent standard error ($n = 3$).

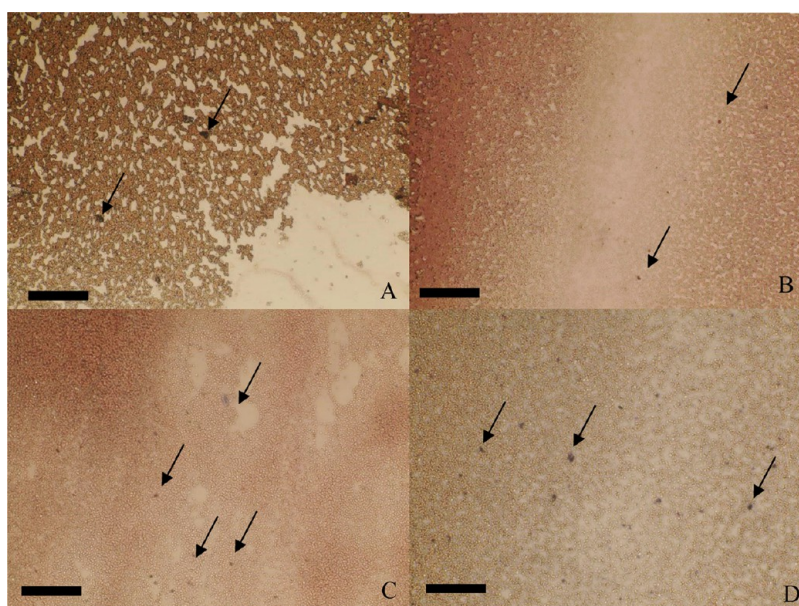


Figure 6. Smear images of whole blood after exposure to sponges for 3 min and staining with Leishman stain. All images are in 10× magnification. (A) Ch/PVA/G(Cl) sponge showing minimal platelet aggregation (arrows). (B) Ch/PVA/G(Cl)-AB sponge showing small platelet aggregation. (C) Ch/PVA/G(Cl)-HA sponge showing multiple and sporadic platelet aggregations. (D) Ch/PVA/G(Cl)-HA-AB sponge showing multiple platelet aggregations. All scale bar is at 200 μm .

Evaluation of the Swelling. The swelling ability of the developed sponges, Ch/PVA/G(Cl), Ch/PVA/G(Cl)-AB, Ch/PVA/G(Cl)-HA, and Ch/PVA/G(Cl)-HA-AB, was tested for their ability to swell in PBS solution.

As shown in Figure 5, the Ch/PVA/G(Cl) sponges exhibited a maximum swelling ability that reached 800%. However, the swelling ability decreased in the rest of the sponge derivatives relative to Ch/PVA/G(Cl). The minimum swelling ability was recorded for the Ch/PVA/G(Cl)-HA as 400% of its mass. This reduction in swelling is due to the morphological analysis of the developed sponges (Figure 2), where the Ch/PVA/G(Cl)-HA sponges demonstrated the lowest porosity, reaching almost half the porosity of the other developed sponges. Moreover, the good crystalline structure observed for the Ch/PVA/G(Cl)-HA could hinder the swelling property of the sponge.³⁹

On the other hand, the AB-loaded sponges displayed a better swelling profile than those loaded with HA. This could be attributed to the release of the ciprofloxacin from the sponges upon immersion in PBS, allowing more water to enter the sponge. Such an effect was confirmed by the enhancement of the swelling profile of the AB-loaded sponges at 20 min, where with the increases in immersion time, more AB is allowed to be released and dissolved. The Ch/PVA/G(Cl)-HA-AB displayed a swelling profile (600%) similar to the Ch/PVA/G(Cl)-AB (750%) at 20 min and better swelling ability than the Ch/PVA/G(Cl)-HA (410%). Although XRD graphs show that Ch/PVA/G(Cl)-HA-AB has the highest crystalline form, it has a better porosity profile, and because ciprofloxacin can chelate Ca^{2+} and is released in the medium during the swelling process, it allows Ch/PVA/G(Cl)-HA-AB to exhibit enhanced swelling ability.^{34,35,40} Such swelling ability is crucial

as it imparts enhanced ability of the developed sponges to absorb blood. The Ch/PVA/G(Cl)-HA-AB sponge, despite being loaded with two materials, still maintains a swelling ability of 600% after 20 min.

The degradation of the sponges was assessed after 1 and 7 days of soaking in PBS. About 60% of the sponge's original mass was degraded after the 1st day. Total loss of mass was 70% after 7 days, indicating the fast release of ciprofloxacin during the first day, followed by very slow sponge degradation (and slow release of the antibiotic) up to the 7th day. Hence, for assessing the antibacterial and cytotoxic effects of the sponges, they were only left for 24 h immersed in any medium.

Hemostatic Effects of Sponges. The hemostatic ability of the developed sponges was examined by observing the interaction of blood upon contact with the sponge. In the case of the Ch/PVA/G(Cl) sponges, the RBCs seem to be fused together without much platelet aggregation, as shown in Figure 6a. Such a response is due to the positive charge on the surface of chitosan, which electrostatically interacts with the negative charge on the RBC surface, thus causing the RBCs to fuse together forming clots.⁴¹

The Ch/PVA/G(Cl)-HA sponge showed the highest platelet aggregation, where multiple sporadic platelet aggregations were observed (Figure 6c). This is due to the ability of the Ca^{2+} present in the HA to initiate the coagulation cascade of blood.⁴² As for Ch/PVA/G(Cl)-AB, platelet aggregates were very few, with fused RBCs seen in the blood smear (Figure 6b). Although ciprofloxacin does not trigger the coagulation cascade per se, it relies on other coagulation factors to enhance coagulopathy.⁴³

The combination of AB and HA within the Ch/PVA/G(Cl)-HA-AB sponges allowed some enhancement of aggregation as compared to the Ch/PVA/G(Cl)-AB due to the positive effect of HA on platelet aggregation.

The hemostatic activity of the developed sponges was further evaluated via quantitative measurement of the reduction in the platelet count after contact with the sponge. A significant decrease in platelet counts (initial count of 610,000/well) was observed for all sponges from 1 to 3 min (Figure 7).

The Ch/PVA/G(Cl)-HA sponges demonstrated the highest platelet aggregation ability, where the number of platelets was reduced to 60,000 platelets per well after 1 min of contact.

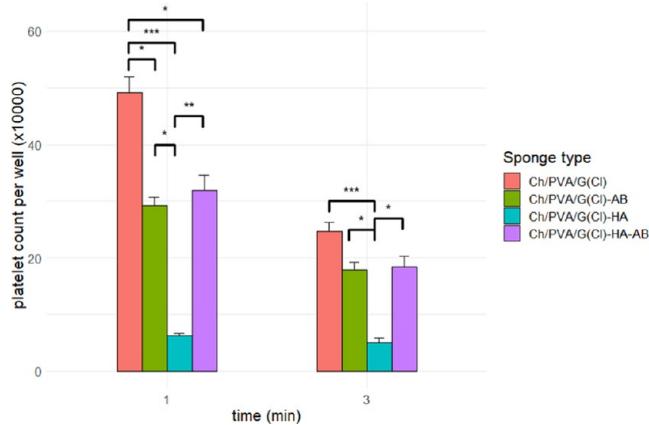


Figure 7. Platelet count of sponges that are in contact with platelet-rich plasma for 1 and 3 min. Error bars represent standard error ($n = 3$). * p -value < 0.05, ** p -value < 0.01, *** p -value < 0.001.

This is due to the presence of Ca^{2+} in the HA within the Ch/PVA/G(Cl)-HA sponges, which binds to dense bodies inside the platelets, releasing coagulation factors and more Ca^{2+} ions outside, allowing more platelets to undergo the same pattern.^{42,44}

The Ch/PVA/G(Cl) sponge demonstrated the lowest platelet aggregation ability, as chitosan tends to attract and fuse RBCs rather than platelets.⁴⁵ On the other hand, both Ch/PVA/G(Cl)-AB and Ch/PVA/G(Cl)-HA-AB showed a similar and enhanced platelet aggregation ability as compared to the Ch/PVA/G(Cl) after 1 and 3 min of contact (p -value = 0.591, 0.923). Such similar behavior could be attributed to the chelation ability of ciprofloxacin toward Ca^{2+} , thus hindering the platelet coagulation cascade caused via HA.^{34,35,40} Still, some enhancement in the platelet aggregation, especially after 1 min, was observed for the Ch/PVA/G(Cl)-HA-AB as compared to the Ch/PVA/G(Cl)-AB.

Antibacterial Disk Diffusion Method. The disk diffusion method was utilized for antibacterial evaluation of the antimicrobial ability of the developed sponges against three different bacterial species, namely, *E. coli*, *S. aureus*, and *P. aeruginosa*. To study the effect of the sponges in different sizes and thus concentrations of the loaded materials, the sponges were cut into 5.5 mm disks, and then the disks were further cut in half and quarter disks (equivalent diameters of 2.25 and 1.125 mm, respectively). The full set of masses of each component is represented in Table 1.

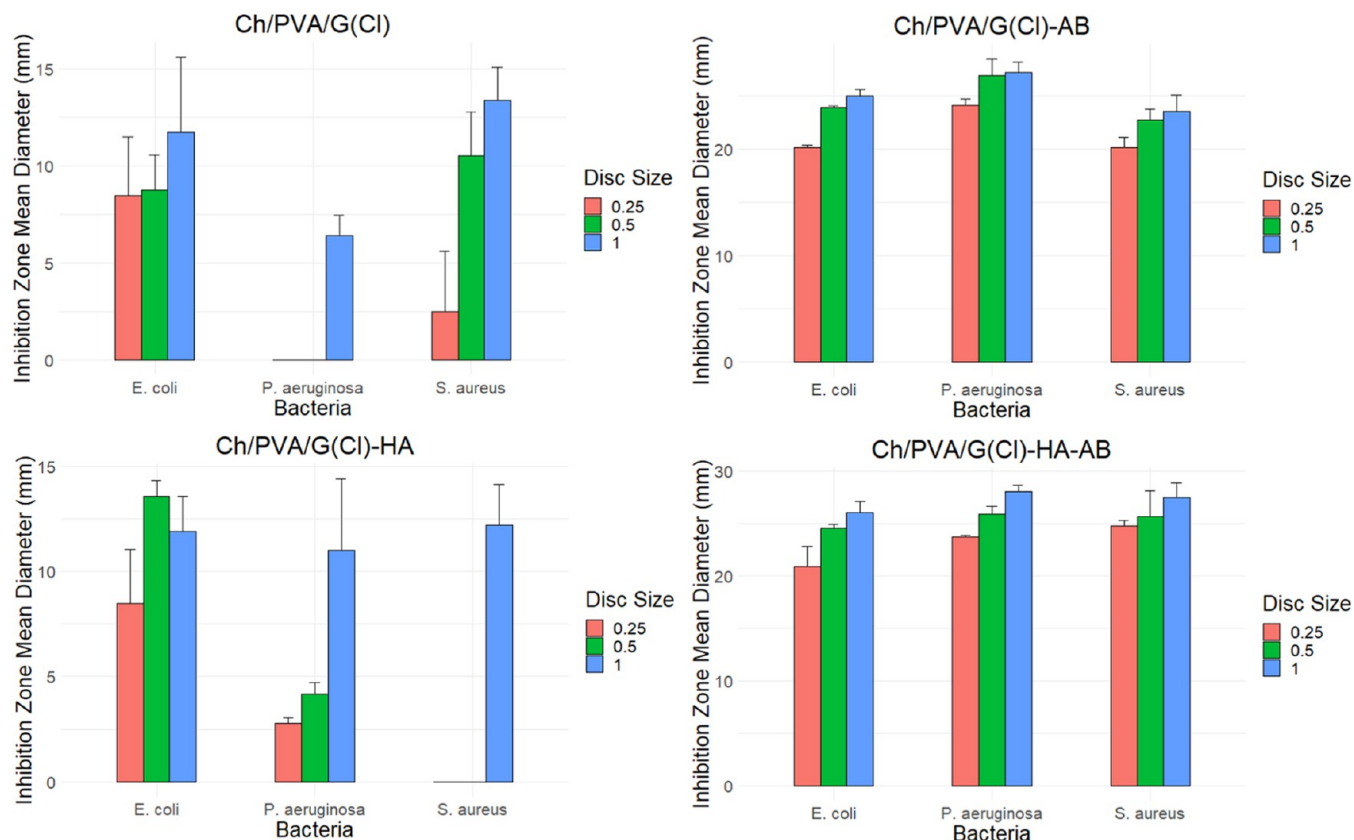
Ch/PVA/G(Cl) exhibited the lowest antibacterial activity against *P. aeruginosa*, *E. coli*, and *S. aureus*, with inhibition zones of 6.4, 11.74, and 13.4 mm, respectively (Figure 8). Chitosan exhibits antibacterial property where the positive charge on the polymer chains of chitosan binds electrostatically to the negatively charged cell walls of bacteria. This would lead to disruption in the cell membrane, leaking the DNA out of the matrix and binding with chitosan, inhibiting DNA replication, and causing bacterial death.^{46–48} Hence, chitosan has inherent antibacterial properties, and since the sponges degrade rapidly within the first 24 h, chitosan can diffuse outward from the disk and cause the inhibition zone observed (Figure 9).

The addition of ciprofloxacin, as a broad-spectrum antibiotic, in Ch/PVA/G(Cl)-AB, leads to an increase in antibacterial activity against all tested bacteria. The inhibition zone increased significantly when tested against *P. aeruginosa*, up to 27.24 mm (p -value = 0.02). The observed antibacterial activity of Ch/PVA/G(Cl)-AB against *S. aureus* and *E. coli* is similar to that found commonly in the literature.⁴⁹ Ciprofloxacin disrupts topoisomerase II, which is responsible for untangling the DNA during replication, thus leading to the prevention of DNA replication due to the supercoiling of DNA.³⁵

The Ch/PVA/G(Cl)-HA exhibited comparable antibacterial activity across all bacteria, with the exception of *S. aureus*. Inhibition of *S. aureus* was only observed when the content of Ch/PVA/G(Cl)-HA was 146 μg (the full-size disk). HA, within the Ch/PVA/G(Cl)-HA, has two pathways to induce bactericidal effect: in the first pathway, Ca^{2+} ion stress is induced, and the ions disrupt the cell membrane of the bacteria.⁵⁰ In the second pathway, the hydroxyapatite generates superoxide species on the surface of HA, thus disrupting the bacterial cell wall upon contact.⁵¹ Since *S. aureus* can produce catalase enzyme, which breaks down superoxide species, the only other pathway to induce bactericidal effect would be to induce Ca^{2+} stress, which induces disruption in the cell wall of

Table 1. Mass of Ch/PVA/G(Cl) Sponges and Their Derivatives in mg

sponge type	mass of disk ϕ 5.5 mm (mg)	Ch (mg)	PVA (mg)	ciprofloxacin (mg)	HA (mg)
Ch/PVA/G(Cl)	8.3	2.075	2.075		
Ch/PVA/G(Cl)-AB	5.05	1.26	1.26	0.25	
Ch/PVA/G(Cl)-HA	2.875	0.72	0.72		0.14
Ch/PVA/G(Cl)-HA-AB	4.475	1.12	1.12	0.22	0.22

**Figure 8.** Inhibition zones of *P. aeruginosa*, *E. coli*, and *S. aureus* against the four sponge types Ch/PVA/G(Cl), Ch/PVA/G(Cl)-AB, Ch/PVA/G(Cl)-HA, and Ch/PVA/G(Cl)-HA-AB. The error bars represent standard error bars ($n = 3$).

S. aureus, and such an effect could not be realized except at the full-size disk of the hemostatic sponge as the concentration is sufficient to induce the antibacterial effect (Figure 9).^{50,52}

Ch/PVA/G(Cl)-HA-AB exhibited the strongest antibacterial activity against all bacterial species. Ciprofloxacin, being homogeneously distributed with HA, will chelate Ca^{2+} ions. This chelation will result in delivering Ca^{2+} ions inside the matrix of the bacteria instead of being inside the vesicles on their membranes, thus preventing the efflux of ciprofloxacin out of the bacteria or degradation by bacterial enzymes. Moreover, the chelation of Ca^{2+} by ciprofloxacin may change the antibiotic structure, thereby preventing the possible acetyl modification that virulent bacterial strains produce to inhibit antibiotic effects.

Sponges containing ciprofloxacin (Ch/PVA/G(Cl)-AB and Ch/PVA/G(Cl)-HA-AB) showed significant statistical differences in their antibacterial activities as compared to blanks or sponges containing only HA (Figure 8).

Cytotoxicity of the Developed Sponges. The cytotoxicity of sponges was examined within 24 h of incubation with fibroblasts (L929). Different sizes and concentrations of the loaded materials were examined for their cytotoxicity. The developed sponges Ch/PVA/G(Cl), Ch/PVA/G(Cl)-AB, Ch/

PVA/G(Cl)-HA, and Ch/PVA/G(Cl)-HA-AB exhibited different cytotoxic activities against fibroblasts. Ch/PVA/G(Cl) and Ch/PVA/G(Cl)-HA showed the least cytotoxicity among other derivative sponges. These outcomes agree with previous reports, where the addition of HA to scaffolds enhanced the proliferation of cells and even, in some cases, differentiation of mesenchymal stem cells or osteogenic progenitor cells to osteoblasts.^{53–56}

Both Ch/PVA/G(Cl)-AB and Ch/PVA/G(Cl)-HA-AB showed 50% viability toward normal cells. However, upon reducing the disk size, the content of the sponges reduced to half, where both Ch/PVA/G(Cl)-AB and Ch/PVA/G(Cl)-HA-AB exhibited normal viability toward L929 cells. Although ciprofloxacin exhibits strong cytotoxicity toward mammalian cells, ciprofloxacin will still be effective and safe at half the concentration with reduced disk sizes, as shown in Figure 10.

CONCLUSIONS

Biocompatible multifunctional hemostatic sponges were developed, which also exhibit strong antibacterial activity, good mechanical properties, and pronounced hemostatic activity. Gelatin/dopamine cryogels were prepared to stop deep noncompressible hemorrhage.⁵⁵ Additionally, quater-

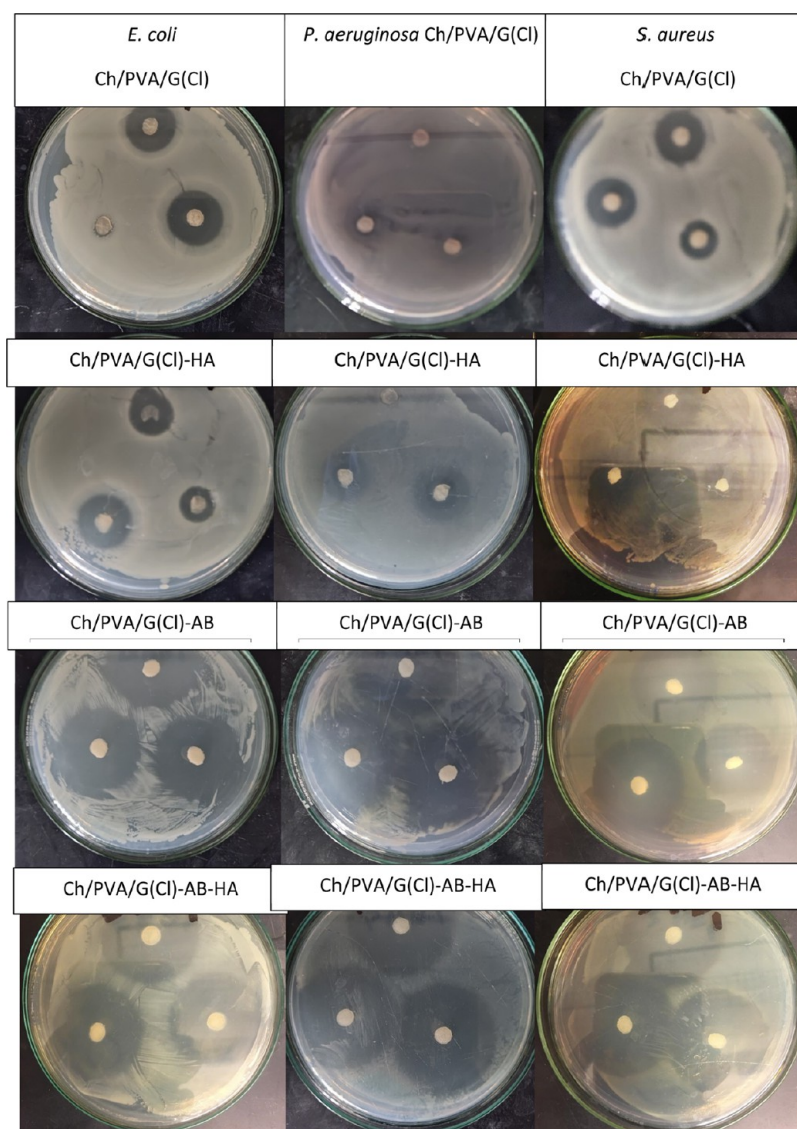


Figure 9. Antibacterial assay of the developed sponges utilizing the disk diffusion method. ($n = 3$). The scale bar in white is 10 mm.

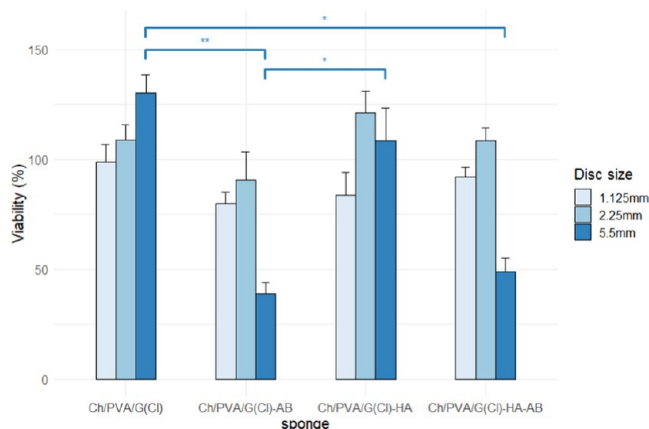


Figure 10. MTT assay of the sponge extract showing that antibiotic activity had a major effect on cell cytotoxicity. Kruskal–Wallis and Dunn tests ($n = 3$). * p -value < 0.05 , ** p -value < 0.01 .

nized chitosan and polydopamine cryogels were prepared to stop surface hemorrhage.⁵⁶ Chitosan-based sponges developed in this study have strong antibacterial properties and can

support bone tissue regeneration due to the loaded ciprofloxacin and HA, respectively. The mechanical tests demonstrated the need to add PVA and glycerol to the chitosan sponges in addition to a crosslinking agent, where their addition allowed the enhancement of the tensile strength and elastic modulus of the sponges. Ch/PVA/G(Cl) was selected as the basic sponge material, which was further loaded with HA and AB and their combination to develop the multifunctional hemostatic sponge. For clinical applications, the biodegradability and inflammatory responses of the prepared sponges should be assessed in hemostatic animal models.

Ch/PVA/G(Cl)-HA demonstrated the strongest platelet aggregation activity and good cell viability; however, it exhibited poor mechanical properties and poor antibacterial activity, especially against *S. aureus*.

On the other hand, both the Ch/PVA/G(Cl)-AB and Ch/PVA/G(Cl)-HA-AB demonstrated enhanced mechanical properties. However, the Ch/PVA/G(Cl)-AB exhibited high cytotoxicity. In contrast, the Ch/PVA/G(Cl)-HA-AB exhibited enhanced cell viability, swelling properties, and platelet aggregation ability. The Ch/PVA/G(Cl)-HA-AB exhibited

the strongest antibacterial activity among all of the prepared sponges due to the chelation of Ca²⁺ ions within the HA by ciprofloxacin. Therefore, the developed Ch/PVA/G(Cl)-HA-AB sponges are proposed as multifunctional homeostatic sponges, which demonstrated strong antibacterial activity against *E. coli*, *S. aureus*, and *P. aeruginosa*, low cytotoxicity, enhanced platelet aggregation and swelling capabilities, and good mechanical properties with possible application in dental and bone surgeries.

AUTHOR INFORMATION

Corresponding Authors

Wessam Awad Sarhan – Department of Chemistry, School of Sciences and Engineering, The American University in Cairo, New Cairo, Cairo 11835, Egypt; Email: wesamawad@aucegypt.edu

Hassan M. E. Azzazy – Department of Chemistry, School of Sciences and Engineering, The American University in Cairo, New Cairo, Cairo 11835, Egypt; Email: hazzazy@aucegypt.edu

Authors

Saif El-Din Al-Mofty – Department of Chemistry, School of Sciences and Engineering, The American University in Cairo, New Cairo, Cairo 11835, Egypt; orcid.org/0000-0001-7708-7413

Ali H. Karaly – Department of Chemistry, School of Sciences and Engineering, The American University in Cairo, New Cairo, Cairo 11835, Egypt; orcid.org/0000-0002-1711-5862

Complete contact information is available at: <https://pubs.acs.org/10.1021/acsomega.2c00654>

Author Contributions

The manuscript was written through contributions of all authors. All authors have given approval to the final version of the manuscript.

Notes

The authors declare the following competing financial interest(s): Wessam Awad Sarhan, Mousa S. Salem, and Hassan M. E. Azzazy are listed as co-inventors on a hemostatic sponge patent submitted to USPTO.

ACKNOWLEDGMENTS

This work has been funded by a grant from the American University in Cairo to HMEA.

ABBREVIATIONS

Ch, Chitosan; PVA, poly(vinyl alcohol); G, Glycerol; (Cl), crosslinked; HA, hydroxyapatite; AB, antibiotic (ciprofloxacin); Ch/PVA/G(Cl), crosslinked sponges with citric acid; Ch/PVA/G(Cl)-AB, crosslinked sponges with ciprofloxacin; Ch/PVA/G(Cl)-HA, crosslinked sponges with hydroxyapatite; Ch/PVA/G(Cl)-HA-AB, crosslinked sponges with hydroxyapatite and ciprofloxacin; *E. coli*, *Escherichia coli*; *S. aureus*, *Staphylococcus aureus*; *P. aeruginosa*, *Pseudomonas aeruginosa*; MTT, 3-(4,5-dimethylthiazol-2-yl)-2,5-diphenyltetrazolium; EDTA, ethylene diamine tetra acetic acid; SEM, Scanning electron microscope; FTIR, Fourier transform infrared spectroscopy; UTM, universal tensile machine

REFERENCES

- (1) Kauvar, D. S.; Lefering, R.; Wade, C. E. Impact of hemorrhage on trauma outcome: an overview of epidemiology, clinical presentations, and therapeutic considerations. *J. Trauma Acute Care Surg.* **2006**, *60*, S3–S11.
- (2) Guo, B.; Dong, R.; Liang, Y.; Li, M. Haemostatic materials for wound healing applications. *Nat. Rev. Chem.* **2021**, *5*, 773–791.
- (3) Rustagi, T.; Patel, K.; Kadrekar, S.; Jain, A. Oxidized Cellulose (Surgicel) Causing Postoperative Cauda Equine Syndrome. *Cureus* **2017**, *9*, No. e1500.
- (4) Habal, P.; Omran, N.; Mand'ák, J.; Simek, J.; Stetina, M. Controlled hemostasis in thoracic surgery using drugs with oxidized cellulose. *Acta Med.* **2011**, *54*, 153.
- (5) Aguilar, A.; Zein, N.; Harmouch, E.; Hafdi, B.; Bornert, F.; Offner, D.; Clauss, F.; Fioretti, F.; Huck, O.; Benkirane-Jessel, N. Application of chitosan in bone and dental engineering. *Molecules* **2019**, *24*, No. 3009.
- (6) Wang, X.; Yan, Y.; Zhang, R. A comparison of chitosan and collagen sponges as hemostatic dressings. *J. Bioact. Compat. Polym.* **2006**, *21*, 39–54.
- (7) Di Martino, A.; Sittinger, M.; Risbud, M. V. Chitosan: a versatile biopolymer for orthopaedic tissue-engineering. *Biomaterials* **2005**, *26*, 5983–5990.
- (8) Nettles, D. L.; Elder, S. H.; Gilbert, J. A. Potential use of chitosan as a cell scaffold material for cartilage tissue engineering. *Tissue Eng.* **2002**, *8*, 1009–1016.
- (9) Francis Suh, J.-K.; Matthew, H. W. Application of chitosan-based polysaccharide biomaterials in cartilage tissue engineering: a review. *Biomaterials* **2000**, *21*, 2589–2598.
- (10) Pineda-Castillo, S.; Bernal-Ballén, A.; Bernal-López, C.; Segura-Puello, H.; Nieto-Mosquera, D.; Villamil-Ballesteros, A.; Muñoz-Forero, D.; Munster, L. Synthesis and characterization of poly(vinyl alcohol)-chitosan-hydroxyapatite scaffolds: a promising alternative for bone tissue regeneration. *Molecules* **2018**, *23*, 2414.
- (11) Zhang, W.; Yang, Y.; Zhang, K.; Luo, T.; Tang, L.; Li, Y. Silk-Poly (lactic-co-glycolic acid) Scaffold/Mesenchymal Stem Cell Composites for Anterior Cruciate Ligament Reconstruction in Rabbits. *J. Biomater. Tissue Eng.* **2017**, *7*, 571–581.
- (12) Teodorescu, M.; Bercea, M.; Morariu, S. Biomaterials of PVA and PVP in medical and pharmaceutical applications: Perspectives and challenges. *Biotechnol. Adv.* **2019**, *37*, 109–131.
- (13) Nakayama, Y.; Takatsuka, M.; Matsuda, T. Surface Hydrogelation Using Photolysis of Dithiocarbamate or Xanthate: Hydrogelation, Surface Fixation, and Bioactive Substance Immobilization. *Langmuir* **1999**, *15*, 1667–1672.
- (14) Pinto, E. P.; Tavares, W. d. S.; Matos, R. S.; Ferreira, A. M.; Menezes, R. P.; Costa, M. E. H. M. d.; Souza, T. M. d.; Ferreira, I. M.; Sousa, F. F. O. d.; Zamora, R. R. M. Influence of low and high glycerol concentrations on wettability and flexibility of chitosan biofilms. *Química Nova* **2018**, *41*, 1109–1116.
- (15) Thiebaud, S.; Aburto, J.; Alric, I.; Borredon, E.; Bikiaris, D.; Prinos, J.; Panayiotou, C. Properties of fatty-acid esters of starch and their blends with LDPE. *J. Appl. Polym. Sci.* **1997**, *65*, 705–721.
- (16) Danilchenko, S. N.; Kalinkevich, O. V.; Pogorelov, M. V.; Kalinkevich, A. N.; Sklyar, A. M.; Kalinichenko, T. G.; Ilyashenko, V. Y.; Starikov, V. V.; Bumeyster, V. I.; Sikora, V. Z.; Sukhodub, L. F. Characterization and in vivo evaluation of chitosan-hydroxyapatite bone scaffolds made by one step coprecipitation method. *J. Biomed. Mater. Res. Part A* **2011**, *96A*, 639–647.
- (17) Zhang, X.; Zhu, L.; Lv, H.; Cao, Y.; Liu, Y.; Xu, Y.; Ye, W.; Wang, J. Repair of rabbit femoral condyle bone defects with injectable nanohydroxyapatite/chitosan composites. *J. Mater. Sci.: Mater. Med.* **2012**, *23*, 1941–1949.
- (18) Gaihre, B.; Jayasuriya, A. C. Comparative investigation of porous nano-hydroxyapatite/chitosan, nano-zirconia/chitosan and novel nano-calcium zirconate/chitosan composite scaffolds for their potential applications in bone regeneration. *Mater. Sci. Eng. C* **2018**, *91*, 330–339.

- (19) Rosen, B. P.; McClees, J. S. Active transport of calcium in inverted membrane vesicles of *Escherichia coli*. *Proc. Natl. Acad. Sci. U.S.A.* **1974**, *71*, 5042–5046.
- (20) Mohammadi, Z. Systemic, prophylactic and local applications of antimicrobials in endodontics: an update review. *Int. Dent. J.* **2009**, *59*, 175–186.
- (21) Mavroidi, A.; Miriagou, V.; Liakopoulos, A.; Tzelepi, E.; Stefanos, A.; Dalekos, G. N.; Petinaki, E. Ciprofloxacin-resistant *Escherichia coli* in Central Greece: mechanisms of resistance and molecular identification. *BMC Infect. Dis.* **2012**, *12*, No. 371.
- (22) Mandal, J.; Acharya, N. S.; Buddhapriya, D.; Parija, S. C. Antibiotic resistance pattern among common bacterial uropathogens with a special reference to ciprofloxacin resistant *Escherichia coli*. *Indian J. Med. Res.* **2012**, *136*, 842–849.
- (23) Ma, X.; Wang, Y.; Guo, H.; Wang, J. Nano-hydroxyapatite/chitosan sponge-like biocomposite for repairing of rat calvarial critical-sized bone defect. *J. Bioact. Compat. Polym.* **2011**, *26*, 335–346.
- (24) Bhargav, H.; Shastri, S. D.; Poornav, S.; Darshan, K.; Nayak, M. M. In *Measurement of the Zone of Inhibition of an Antibiotic*, 2016 IEEE 6th International Conference on Advanced Computing (IACC); IEEE, 2016; pp 409–414.
- (25) Cleveland, W. S.; Grosse, E.; Shyu, W. M. In *Local Regression Models. Chapter 8 in Statistical Models in S*; Chambers, J. M.; Hastie, T. J., Eds.; Wadsworth & Brooks/Cole: Pacific Grove, CA, 1992; p 608.
- (26) Abraham, A.; Soloman, P. A.; Rejini, V. O. Preparation of chitosan-polyvinyl alcohol blends and studies on thermal and mechanical properties. *Procedia Technol.* **2016**, *24*, 741–748.
- (27) Mohsin, M.; Hossin, A.; Haik, Y. Thermal and mechanical properties of poly(vinyl alcohol) plasticized with glycerol. *J. Appl. Polym. Sci.* **2011**, *122*, 3102–3109.
- (28) Abraham, A.; Soloman, P. A.; Rejini, V. O. Preparation of Chitosan-Polyvinyl Alcohol Blends and Studies on Thermal and Mechanical Properties. *Procedia Technol.* **2016**, *24*, 741–748.
- (29) Lipatova, I. M.; Yusova, A. A. Effect of mechanical activation on starch crosslinking with citric acid. *Int. J. Biol. Macromol.* **2021**, *185*, 688–695.
- (30) Jiang, L.; Li, Y.; Wang, X.; Zhang, L.; Wen, J.; Gong, M. Preparation and properties of nano-hydroxyapatite/chitosan/carboxymethyl cellulose composite scaffold. *Carbohydr. Polym.* **2008**, *74*, 680–684.
- (31) Neiva, E. G.; Bergamini, M. F.; Oliveira, M. M.; Marcolino, L. H., Jr; Zarbin, A. J. PVP-capped nickel nanoparticles: synthesis, characterization and utilization as a glycerol electrosensor. *Sens. Actuators, B* **2014**, *196*, 574–581.
- (32) Frost, R. W.; Lassetter, K.; Noe, A.; Shamblen, E.; Lettieri, J. Effects of aluminum hydroxide and calcium carbonate antacids on the bioavailability of ciprofloxacin. *Antimicrob. Agents Chemother.* **1992**, *36*, 830–832.
- (33) Kara, M.; Hasinoff, B.; McKay, D.; Campbell, N. Clinical and chemical interactions between iron preparations and ciprofloxacin. *Br. J. Clin. Pharmacol.* **1991**, *31*, 257–261.
- (34) Uivarosi, V. Metal complexes of quinolone antibiotics and their applications: an update. *Molecules* **2013**, *18*, 11153–11197.
- (35) Zhang, Y.; Wang, Q. S.; Yan, K.; Qi, Y.; Wang, G. F.; Cui, Y. L. Preparation, characterization, and evaluation of genipin crosslinked chitosan/gelatin three-dimensional scaffolds for liver tissue engineering applications. *J. Biomed. Mater. Res., Part A* **2016**, *104*, 1863–1870.
- (36) Turel, I.; Bukovec, P. Comparison of the thermal stability of ciprofloxacin and its compounds. *Thermochim. Acta* **1996**, *287*, 311–318.
- (37) Bitter, J. Effect of crystallinity and swelling on the permeability and selectivity of polymer membranes. *Desalination* **1984**, *51*, 19–35.
- (38) Neuvonen, P. J.; Kivistö, K. T.; Lehto, P. Interference of dairy products with the absorption of ciprofloxacin. *Clin. Pharmacol. Ther.* **1991**, *50*, 498–502.
- (39) Okamoto, Y.; Yano, R.; Miyatake, K.; Tomohiro, I.; Shigemasa, Y.; Minami, S. Effects of chitin and chitosan on blood coagulation. *Carbohydr. Polym.* **2003**, *53*, 337–342.
- (40) Silver, M. J. Role of calcium ions and phospholipids in platelet aggregation and plug formation. *Am. J. Physiol. Legacy Content* **1965**, *209*, 1128–1136.
- (41) Israel, D. S.; Stotka, J.; Rock, W.; Sintek, C. D.; Kamada, A. K.; Klein, C.; Swaim, W. R.; Pluhar, R. E.; Toscano, J. P.; Lettieri, J. T.; et al. Effect of ciprofloxacin on the pharmacokinetics and pharmacodynamics of warfarin. *Clin. Infect. Dis.* **1996**, *22*, 251–256.
- (42) Massini, P.; Käser-Glanzmann, R.; Lüscher, E. F. Movement of calcium ions and their role in the activation of platelets. *Thromb. Haemostasis* **1978**, *40*, 212–218.
- (43) Matica, A.; Aachmann; Tøndervik; Sletta, H.; Ostafe. Chitosan as a Wound Dressing Starting Material: Antimicrobial Properties and Mode of Action. *Int. J. Mol. Sci.* **2019**, *20*, 5889.
- (44) Balouiri, M.; Sadiki, M.; Ibsouda, S. K. Methods for in vitro evaluating antimicrobial activity: A review. *J. Pharm. Anal.* **2016**, *6*, 71–79.
- (45) Patel, J. B.; Cockerill, F.; Bradford, P. A. Performance standards for antimicrobial susceptibility testing: twenty-fifth informational supplement, 2015.
- (46) Xie, Y.; Yang, L. Calcium and Magnesium Ions Are Membrane-Active against Stationary-Phase *Staphylococcus aureus* with High Specificity. *Sci. Rep.* **2016**, *6*, No. 20628.
- (47) Ragab, H. S.; Ibrahim, F. A.; Abdallah, F.; Al-Ghamdi, A. A.; El-Tantawy, F.; Radwan, N.; Yakuphanoglu, F. Synthesis and in vitro antibacterial properties of hydroxyapatite nanoparticles. *IOSR J. Pharm. Biol. Sci.* **2014**, *9*, 77–85.
- (48) No, H. K.; Park, N. Y.; Lee, S. H.; Meyers, S. P. Antibacterial activity of chitosans and chitosan oligomers with different molecular weights. *Int. J. Food Microbiol.* **2002**, *74*, 65–72.
- (49) Hosseinnejad, M.; Jafari, S. M. Evaluation of different factors affecting antimicrobial properties of chitosan. *Int. J. Biol. Macromol.* **2016**, *85*, 467–475.
- (50) Kanafani, H.; Martin, S. E. Catalase and superoxide dismutase activities in virulent and nonvirulent *Staphylococcus aureus* isolates. *J. Clin. Microbiol.* **1985**, *21*, 607–610.
- (51) Clarke, S.; Choi, S.; McKechnie, M.; Burke, G.; Dunne, N.; Walker, G.; Cunningham, E.; Buchanan, F. Osteogenic cell response to 3-D hydroxyapatite scaffolds developed via replication of natural marine sponges. *J. Mater. Sci.: Mater. Med.* **2016**, *27*, No. 22.
- (52) Peng, L.; Zhou, Y.; Lu, W.; Zhu, W.; Li, Y.; Chen, K.; Zhang, G.; Xu, J.; Deng, Z.; Wang, D. Characterization of a novel polyvinyl alcohol/chitosan porous hydrogel combined with bone marrow mesenchymal stem cells and its application in articular cartilage repair. *BMC Musculoskeletal Disord.* **2019**, *20*, No. 257.
- (53) Li, H.; Zhu, R.; Sun, L.; Xue, Y.; Hao, Z.; Xie, Z.; Fan, X.; Fan, H. Effect of thickness of HA-coating on microporous silk scaffolds using alternate soaking technology. *BioMed Res. Int.* **2014**, *2014*, No. 637821.
- (54) He, P.; Sahoo, S.; Ng, K. S.; Chen, K.; Toh, S. L.; Goh, J. C. H. Enhanced osteoinductivity and osteoconductivity through hydroxyapatite coating of silk-based tissue-engineered ligament scaffold. *J. Biomed. Mater. Res., Part A* **2013**, *101A*, 555–566.
- (55) Huang, Y.; Zhao, X.; Zhang, Z.; Liang, Y.; Yin, Z.; Chen, B.; Bai, L.; Han, Y.; Guo, B. Degradable gelatin-based IPN cryogel hemostat for rapidly stopping deep noncompressible hemorrhage and simultaneously improving wound healing. *Chem. Mater.* **2020**, *32*, 6595–6610.
- (56) Li, M.; Zhang, Z.; Liang, Y.; He, J.; Guo, B. Multifunctional tissue-adhesive cryogel wound dressing for rapid nonpressing surface hemorrhage and wound repair. *ACS Appl. Mater. Interfaces* **2020**, *12*, 35856–35872.